Journal of Alloys and Compounds 509 (2011) 1874–1879

Contents lists available at ScienceDirect

Journal of Alloys and Compounds

journal homepage: www.elsevier.com/locate/jallcom

Effect of melting temperatures on the crystallization and densification of $2.8MgO{\cdot}1.5Al_2O_3{\cdot}5SiO_2$ glass–ceramic synthesized from mainly talc and kaolin

Johar Banjuraizah[a,b], Hasmaliza Mohamad[b], Zainal Arifin Ahmad[b,*]

[a] School of Materials Engineering, Universiti Malaysia Perlis, 02600 Kangar, Perlis, Malaysia
[b] School of Materials and Mineral Resources Engineering, Universiti Sains Malaysia, Engineering Campus, 14300 Nibong Tebal, Penang, Malaysia

ARTICLE INFO

Article history:
Received 7 June 2010
Received in revised form 15 October 2010
Accepted 22 October 2010
Available online 29 October 2010

Keywords:
Temperature of melting
α-Cordierite

ABSTRACT

Single phase α-cordierite with low sintering temperature was produced from $2.8MgO{\cdot}1.5Al_2O_3{\cdot}5SiO_2$ chemical formulation using mainly talc and kaolin. The effect of melting temperature to the densification, crystallization and properties of α-cordierite glass–ceramic was investigated. XRD patterns indicate that, melting at 1350, 1385 and 1400 °C are not sufficient to completely transform the crystalline mixture of compound to fully amorphous phase. DTA peaks demonstrate that the crystallinity of phase, the onset of crystallization temperature, increased as the melting temperature raise. Similar observation trends can be seen from their micrographs, density, dielectric and CTE measurements. Temperature of melting has significantly affected the properties of glass–ceramic.

1. Introduction

α-Cordierite is commonly synthesized using solid state reaction, glass method and sol–gel route. Highly crystalline α-cordierite phase is normally obtained from solid state [1–10] and sol–gel methods [11–18] after sintering above 1000 °C, and below 1000 °C through the glass route [19–28]. However, α-cordierite phase synthesized through the glass route requires the mixture of the compound to be fired above its melting temperature prior to being quenched, pulverized, compacted and sintered. Highly crystalline α-cordierite at low sintering temperatures is essential for multilayer substrates in electronic packaging applications. A majority of researchers following the glass route melted their raw materials above 1500 °C [22,23,25,28–30] to ensure that the compounds were completely transformed into glassy phase. None of the reported studies looked at the effect of temperatures of melting on the quality of synthesized α-cordierite. The reasons for searching for lower melting temperatures would firstly be to reduce energy consumption, thus using low melting furnace and crucibles; and secondly, to minimize the evaporation of certain compounds during melting, such as the fluxing materials. Therefore, any related costs for the production of α-cordierite glass–ceramics can be reduced significantly. For these reasons, the objective of this paper is to study the effect of melting temperatures (from 1350 °C to 1500 °C) on the crystallization and densification of single phase α-cordierite, with formulation $2.8MgO{\cdot}1.5Al_2O_3{\cdot}5SiO_2$ synthesized from mainly talc and kaolin.

2. Experimental procedure

$2.8MgO–1.5Al_2O_3–5SiO_2$ glass–ceramics was synthesized using kaolin (Kaolin Industry, Tapah Perak, Malaysia) and talc (Ipoh Ceramic, Sdn Bhd, Ipoh Malaysia). Silica (Ipoh Ceramic, Sdn Bhd. Ipoh, Malaysia), alumina (Metco, Westbury, USA) and magnesia (Merck, Whitehouse Station, NJ) were added to compensate the formulations of the compositions. The elemental compositions of talc and kaolin were determined by X-ray florescence spectroscopy (Rigaku X-ray spectrometer model RIX 3000) and the details are given in Table 1. Table 2 summarized the detailed compositions of the initial raw materials in weight percent. The homogeneous mixture of compounds was melted at different temperatures (1350 °C, 1385 °C, 1400 °C, 1425 °C, and 1500 °C) in alumina crucibles (Table 3). After 4 h of soaking at the respective temperatures, the samples were immediately quenched in distilled water to form frits, followed by drying to remove moisture. All frits were milled using the same milling parameters to obtain glass powders with average particle sizes in the range of 1–3 μm. The fine glass powders were subjected to XRD and nonisothermal DTA analysis. The glass powders were also pressed and sintered at 900 °C for 2 h with 5 °C/min heating rate. XRD of the sintered pellets was carried out to determine the evolution of the glassy phase to crystalline state. The XRD patterns of the glass and sintered products were obtained using a Bruker D8 Advanced operated in Bragg–Brentano geometry, with Cu Kα radiation, in the $10° \leq 2\theta° \leq 90°$ range. Counting time was fixed at 71.5 s for each 0.03° 2θ step. The X-ray tube was operated at 40 kV and 30 mA. Quantitative phase analysis was measured by Rietveld method using HighScorePlus software. Crystal structure data for each phases present in the samples were taken from ICSD. Global optimized parameters were background coefficient (Chebychev polynomial functions with five orders of the series), lattice parameter, zero-shift error, scale factor, and peak shape parameters. The refinement was done in stages, with the atomic coordination and thermal parameters held fixed. Therefore, Bragg reflection profile (calculated pattern) was calculated by convolution of mathematical functions of these parameters. DTA (Model Linseis) of each glass powder was carried out from room temperature up to 1000 °C with 5 °C/min. CTE test was carried out using high temperature vertical dilatometer tests (Model Linseis) in air from room temperature to 1000 °C, while the dielectric measurements

* Corresponding author. Tel.: +60 012 667 1736; fax: +60 04 594 1011.
E-mail address: zainal@eng.usm.my (Z.A. Ahmad).

0925-8388/$ – see front matter © 2010 Elsevier B.V. All rights reserved.
doi:10.1016/j.jallcom.2010.10.077

Table 1
Elemental analysis of minerals and oxides compound by XRF.

	Kaolin (wt%)	Talc (wt%)	SiO_2 (wt%)	Al_2O_3 (wt%)	MgO (wt%)
MgO	0.88	49	–	–	99
SiO_2	59	47	99.5	0.2	–
Al_2O_3	35	0.16	0.04	99.46	–
K_2O	3	–	–	–	–
CaO	0.014	3	–	0.075	0.13
TiO_2	0.84	–	–	–	–
Fe_2O_3	0.6	0.45	0.04	0.15	0.0036
Cr_2O_3	0.032	–	–	–	–
NiO	0.014	0.028	–	0.022	–
P_2O_5	0.073	0.095	–	–	–
ZrO_2	0.05	–	–	–	–
SO_3	–	0.06	–	–	0.07
CuO	–	0.016	–	0.014	–

Table 2
Weight percent of initial precursors.

Talc	Kaolinite	MgO	Al_2O_3	SiO_2
31	65	3.5845	4.6514	0.904

Table 3
Quantitative analysis of glass powder samples melted at different temperatures.

Melting temperature (°C)	Phases	Quantity (wt%)
1500	Amorphous	100
1425	Amorphous	100
1400	Amorphous	98.40
	α-Cordierite	1.60
1385	Amorphous	91.80
	α-Cordierite	8.90
1350	Amorphous	84.60
	α-Cordierite	14.18
	Spinel	2.22

were made using an Impedance Analyzer (Hewlet Packard model HP4291). Density and porosity of samples were measured using the Archimedes principle.

3. Results and discussions

The XRD patterns of glass powders melted are shown in Fig. 1. XRD patterns confirm that all powders contain an amorphous structure. Samples melted at 1425 °C and 1500 °C are fully amorphous while other samples have a significant amount of crystalline phase, as tabulated in Table 4. Measurement of amorphous content indicates that the percentage of the amorphous phase increased with the increase of melting temperature. Any molten substance will

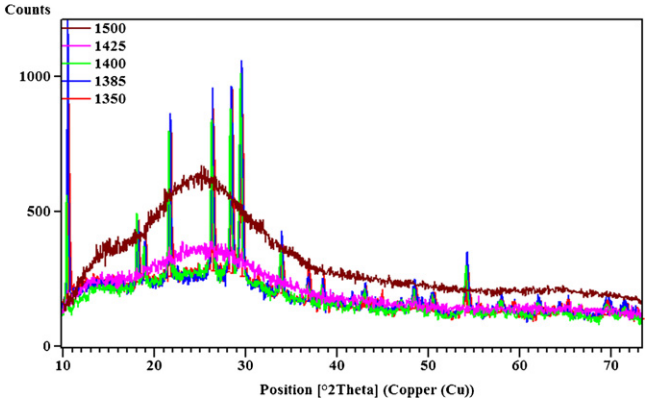

Fig. 1. Diffraction pattern of $2.8MgO{\cdot}1.5Al_2O_3{\cdot}5SiO_2$ composition melted at different melting temperature.

Table 4
Results of Rietveld refinement on $2.8MgO{\cdot}2Al_2O_3{\cdot}5SiO_2$ sintered samples melted at different temperature.

Sample	Phases	Quantity (wt%)	Crystallite size (nm)	R_{wp}	s
1500	α-Cordierite (*P*6/*mcc*)	100	227.7	10.89	2.7
1425	α-Cordierite (*P*6/*mcc*)	99.7	67.9	11.84	3.21
	Silicon oxide/quartz (*P*3121)	0.3			
1400	α-Cordierite (*P*6/*mcc*)	99.2	69.0	10.99	2.52
	Silicon oxide/quartz (*P*3121)	0.8			
1385	α-Cordierite (*P*6/*mcc*)	92	64.5	11.85	2.96
	Silicon oxide/quartz (*P*3121)	6.1			
	Spinel (*Fd*−3*m*)	1.9			
1350	α-Cordierite (*P*6/*mcc*)	88.6	51.8	11.97	3.07
	Silicon oxide/quartz (*P*3121)	6.9			
	Spinel (*Fd*−3*m*)	4.5			

form a glass if it was cooled fast enough. Therefore, melting at a much lower temperature requires the molten glass to be cooled at a sufficiently high rate to avoid a significant degree of crystallization so that the 'disordered' atomic configuration of the liquid state is frozen-in, thus avoiding the formation and growth of crystal embryos.

During heating the mixture of cordierite precursor powders up to 1250 °C, phase transformation will occurs to form α-cordierite phase by solid state reaction. However, the bonding between atoms in α-cordierite structure became weaker as the temperature increases to its melting temperature. At much higher temperature above its melting temperature, some of α-cordierite chain would broke up. Heating the forms of α-cordierite phase exactly to its melting temperature at or just above the softening temperature will cause some of the atoms to remain intact even though the length between the atoms increased. Therefore, melting at and just above melting point will cause some of the atoms to easily revert to the crystalline state, and thus some crystalline phase was observed in the diffraction pattern of the glass powders.

Fig. 2 shows the XRD patterns for samples after heat treatment at 900 °C for 2 h. The plots are divided into three two $2\theta^\circ$ ranges for better observation of the progressive changes of α-cordierite peaks. The dominant crystalline phase for all samples is α-cordierite. Only samples melted at 1500 °C contain single phase α-cordierite. However, samples melted at 1350, 1385 and 1400 °C contain small amounts of spinel and quartz phases.

Quantitative phase analysis of sintered samples was carried out using the Rietveld method and the results are tabulated in Table 2. The convergence was achieved and perfect agreement was observed between measured and calculated patterns for all samples. Fig. 3 demonstrates total weight percent of α-cordierite as a function of melting temperature. The Rietveld results were normalized to 100% of crystalline fraction, so the hypothetical amorphous content of the sample were assumed to be negligible. High purity and single phase α-cordierite were obtained in samples melted at 1425 and 1500 °C. At 1350, 1385 and 1400 °C, small amounts of spinel and quartz were presents in the samples.

Crystallization of amorphous phase was studied using DTA for all samples melted at different temperatures. Fig. 4 shows DTA results of glass under a nonisothermal heat treatment at a constant heating rate of 5 °C/min. Only one exothermic crystallization peak was observed in DTA scans for all samples melted at different temperature. A summary of onset (T_o), peak (T_p), and end (T_f) of crystallization temperatures for all compositions are tabulated in Table 5. As shown in Fig. 4, the exothermic peak weakened as the melting temperature decreased. The area under the exother-

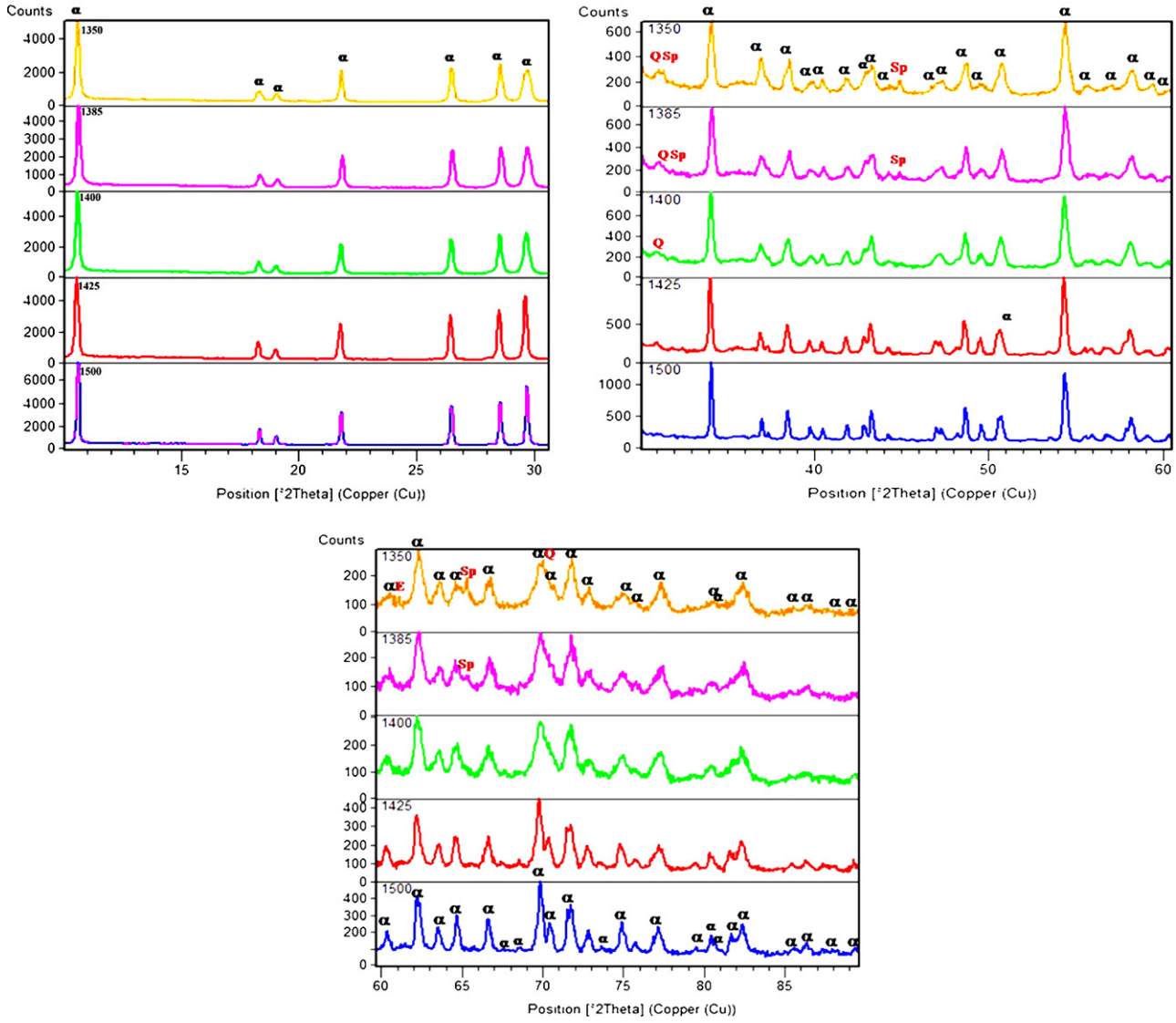

Fig. 2. X-ray diffraction pattern for sintered samples melted at different melting temperature.

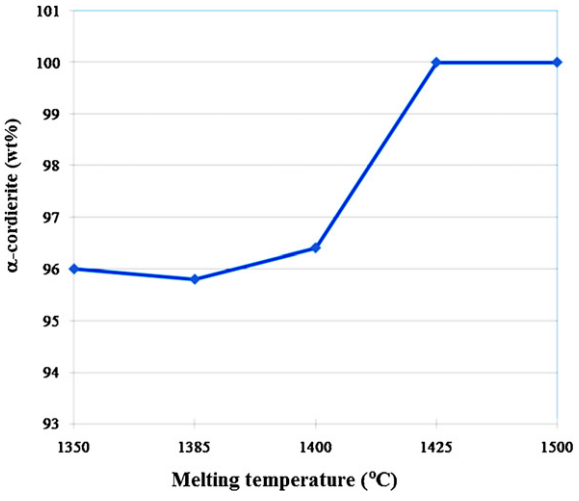

Fig. 3. Weight percent of α-cordierite from total crystalline phase.

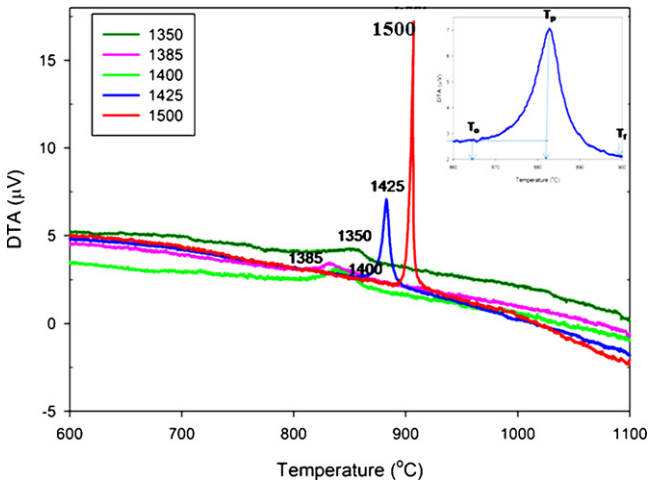

Fig. 4. DTA curves of sample melted at different temperature.

Table 5
Crystallization temperature of samples $2.8MgO{\cdot}1.5Al_2O_3{\cdot}5SiO_2$ glass–ceramic melted at different temperature.

Melting temperature (°C)	T_o (°C)	T_p (°C)	T_f (°C)
1500	889.6	907.4	920.3
1425	854.8	882.6	899.4
1400	812.9	838.9	866.6
1385	806.3	831.4	862.2
1350	823.7	855.9	872.5

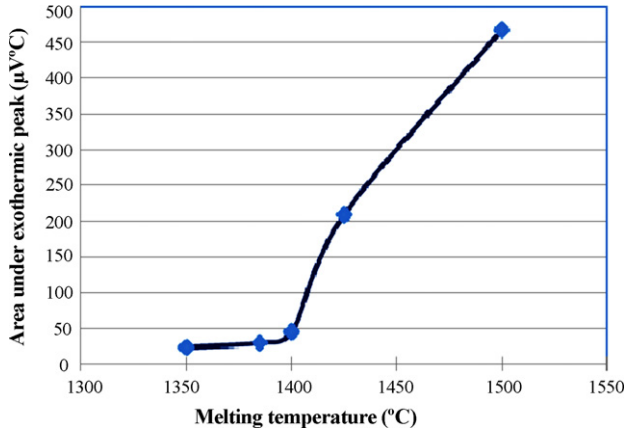

Fig. 5. Area under exothermic peaks for samples melted at different temperature.

mic peak in the DTA curve also indicates the degree of crystallinity. This area was approximated by integrating the baseline at onset and termination of the exothermic to form a triangle. The area under exothermic peak determine the degree of crystallinity, and the trend of crystallinity obtained from DTA analysis, as demonstrated in Fig. 5.

A low dielectric constant is one of the required properties for substrates used in high-speed signals in order to propagate with a shorter delay. Literature reports that the dielectric constant of α-cordierite is 5–6 at 1 MHz [31]. Fig. 6 demonstrates variation of dielectric constant as a function of frequency for samples melted at different temperatures. Dielectric constants were found to decrease with increase in frequency, from 1 MHz to 1.8 GHz, for all samples melted at different temperatures. The slight increase in the dielectric constant at a higher frequency peaking near 1.7 GHz is likely due to dipolar polarization [32]. It is clearly seen in Fig. 7 that there are two distinct groups of dielectric constant values. Samples melted

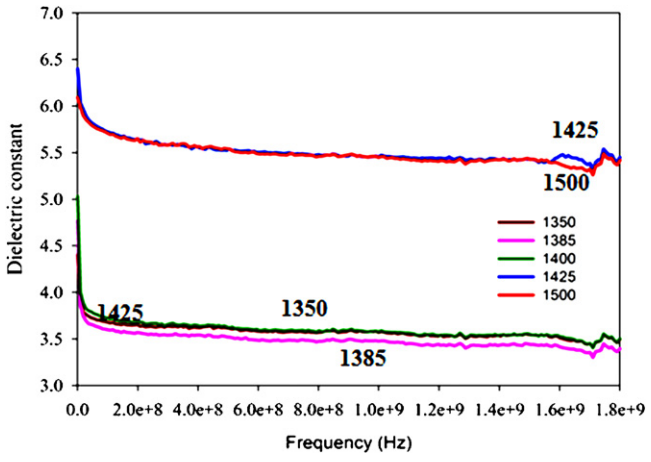

Fig. 6. Dielectric constant of all samples as a function of frequency (1 MHz to 1.8 GHz).

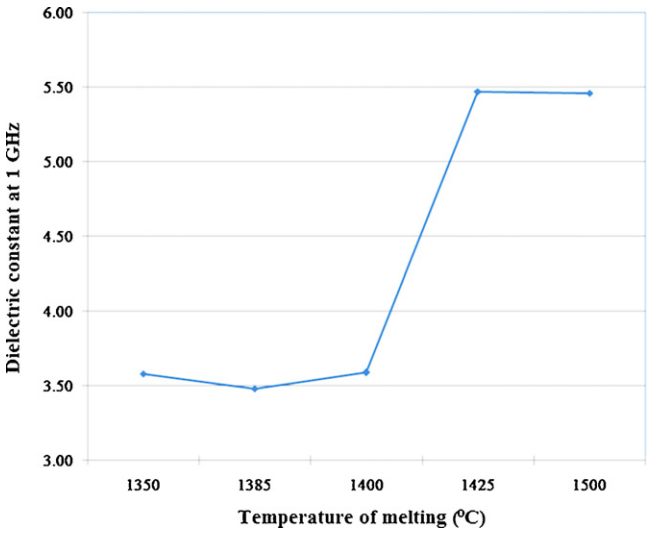

Fig. 7. Effect of melting temperature on dielectric constant measured at frequency 1 GHz.

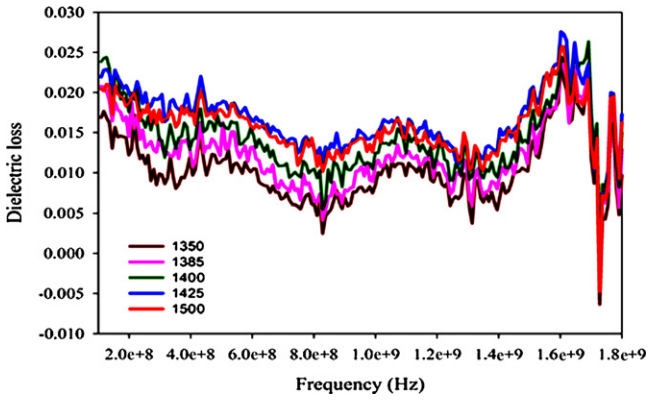

Fig. 8. Dielectric loss of samples melted at different temperature as a function of frequency.

at 1425 and 1500 °C have higher dielectric constants with an average 5.5 which is within the standard. However, samples melted at and below 1400 °C possess lower dielectric constants with an average of 3.5. Dielectric constant is dependent on crystallite size, density and porosity [32]. Lower dielectric constant for samples melted at 1350, 1385 and 1400 °C can be explained by the fact

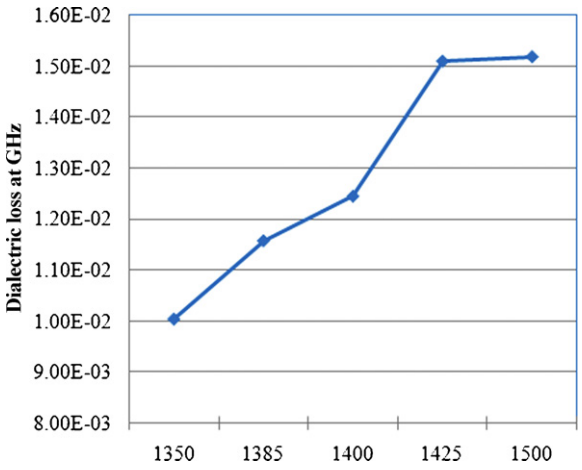

Fig. 9. Effect of temperature of melting to dielectric loss of $2.8MgO{\cdot}1.5Al_2O_3{\cdot}5SiO_2$ glass ceramic.

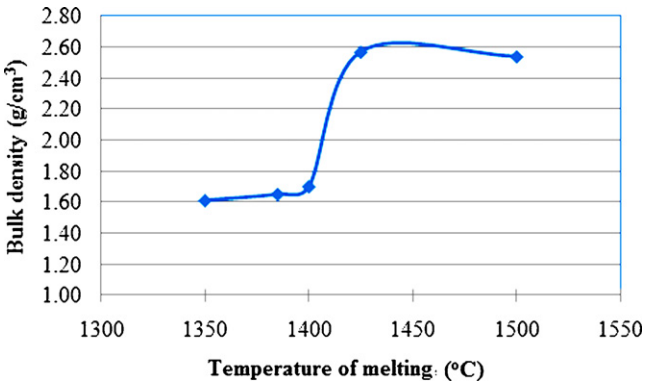

Fig. 10. Bulk density of sintered samples melted at different melting temperature.

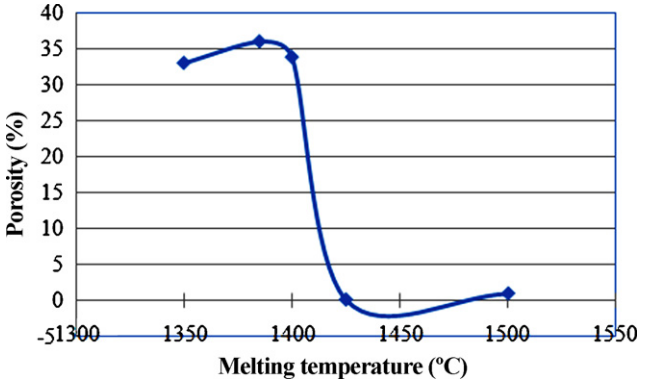

Fig. 11. Percent of porosity in samples melted at different melting temperature.

that the porosity in these samples are higher than the two samples melted at higher melting temperatures. Porosity will significantly affect the dielectric constant. The lower the porosity, the higher the dielectric constant will be. Although by using materials with low dielectric constant, can reduced the delay time can be reduced and thus, increase signal propagation through interconnections which are required in high speed applications, however, the porosity percentage which exist in the sample has to be considered since it will significantly affect the physical properties and can cause current leakage.

Fig. 8 presents variation of dielectric loss as a function of frequency. The dielectric loss values for all samples are within $1–1.5 \times 10^{-2}$ throughout the frequency range. The dielectric loss was found to slightly increase with the increase in temperature of melting, as demonstrated in Fig. 9. The dielectric loss value did not decrease with porosity content, as reported in few literatures [33–35]. Poor densification normally will cause in low dielectric constant and high loss factor. This is in contrast to the results obtained in present study that samples melted at higher temperature which have better densification give low dielectric loss. The trend of dielectric loss of samples as a function of frequency is seems similar to the total amount of amorphous phase that existed in the glass powder samples (Table 3) before heat treated. The impurities that was existed from the initial raw materials was expected to concentrate in the matrix of amorphous glass rather than interstitial inside the crystalline phase that remain in the glass powder samples. During heat treatment or crystallization of the amorphous glass phase, these impurities tend to concentrated in the grain boundaries thus, an increase in polarization will results in high dielectric loss [36].

As demonstrated in Fig. 10, samples that were melted at 1425 and 1500 °C have higher density as compared to samples melted at 1350, 1385 and 1400 °C. This is because samples melted at lower temperatures have higher percentage of porosity, as shown in Fig. 11. This was proved from microstructure analysis on fracture surface, as demonstrated in Fig. 12. Micrograph of samples also indicates that samples melted at lower temperature are partly densified and contain higher porosity as compared to samples melted at 1425 and 1500 °C. Glass powders melted at low melting temperatures contain mixtures of amorphous and polycrystalline phase. Polycrystalline materials are usually sintered by solid state diffusion, while the glass powders are sintered by viscous flow [37]. Therefore, the sintering mechanism in samples melted at low temperatures are expected to occurs by both mechanisms (solid state diffusion and viscous flow), while sample melted at high temperature by viscous flow. Therefore, atomic diffusion processes that occured in sample melted at low temperature which contains the mixture of amorphous and crystalline phase require much high temperature to form bonds between particles. Several parameters that determine the sinterability of these powders are diffusivities, surface and grain boundary energies, average particle size and particle size distribution, particle morphology and green density.

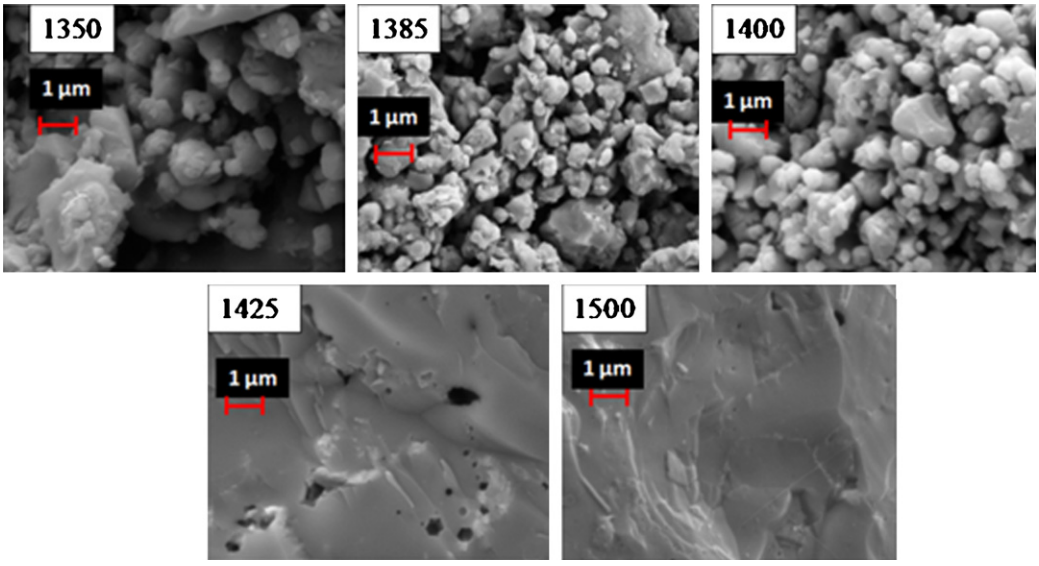

Fig. 12. Microstructure of fracture sample melted at various melting temperature.

Fig. 13. Appearance of glass and glass–ceramic of samples melted at different temperature.

Therefore, in the partly crystalline powder, the diffusivities were difficult to take place at low sintering temperatures, compared to samples with fully amorphous phase. The scarcity of the diffusivities in the partly crystalline powders resulted in low densification. Therefore, samples melted at low temperatures need a significant amount of energy to overcome the lattice energy so that a cation can diffuse into different sites. Samples melted at 1425 °C and 1500 °C, which are in the fully amorphous phase, undergo the viscous flow sintering mechanism allowing them to densify at lower temperatures.

4. Conclusions

The temperature for melting $2.8MgO{\cdot}1.5Al_2O_3{\cdot}5SiO_2$ will influence the characteristic of glass and glass–ceramic properties as demonstrated in Fig. 13. It has been proved that nonstoichiometric cordierite composition synthesized from talc and kaolin could be melted at temperature as low as 1425 °C without devitrification. Melting the composition below this temperatures will result in partly amorphous glass. The existence of small amount of crystalline phase in the matrix of amorphous glass powders will affect the crystallinity of α-cordierite phase that was forms after heat treatment, as well as the densification of the sintered samples. These in turn affect the CTE and dielectric properties of samples. Therefore, it was not suitable for multilayer substrates in high frequency electronic packaging. However, samples melted at and above 1425 °C results in dense structure with high purity and crystallinity of α-cordierite phase at low sintering temperature. In addition, it also possesses low CTE, and dielectric constant, which are comparable to the standard α-cordierite properties synthesized from pure oxides melted above 1500 °C [25,38].

Acknowledgements

The authors gratefully acknowledge the financial support from the Islamic Development Bank and Fundamental Research Grant Scheme (9003-00171) Universiti Malaysia Perlis, and technical assistants from Universiti Sains Malaysia (USM).

References

[1] S. Kurama, H. Kurama, Ceram. Int. 34 (2008) 269–272.
[2] N. Djordjevic, L. Pavlovic, J. Serb. Chem. Soc. 71 (2006) 293–301.
[3] Z.M. Shi, K.M. Liang, S.R. Gu, Mater. Lett. 51 (2001) 68–72.
[4] E. Yalamac, S. Akkurt, Ceram. Int. 32 (2006) 825–832.
[5] R. Goren, H. Gocmez, C. Ozgur, Ceram. Int. 32 (2006) 407–409.
[6] R. Goren, C. Ozgur, H. Gocmez, Ceram. Int. 32 (2006) 53–56.
[7] Z. Acimovic, L. Pavlovic, L. Trumbulovic, L. Andric, M. Stamatovic, Mater. Lett. 57 (2003) 2651–2656.
[8] J.R. Gonzalez-Velasco, R. Ferret, R. Lopez-Fonseca, M.A. Gutierrez-Ortiz, Powder Technol. 153 (2005) 34–42.
[9] S. Tamborenea, A.D. Mazzoni, E.F. Aglietti, Thermochim. Acta 411 (2004) 219–224.
[10] C. Ghitulica, E. Andronescu, O. Nicola, A. Dicea, M. Birsan, J. Eur. Ceram. Soc. 27 (2007) 711–713.
[11] M.K. Naskar, M. Chatterjee, J. Eur. Ceram. Soc. 24 (2004) 3499–3508.
[12] S. Mei, J. Yang, J.M.F. Ferreira, Mater. Res. Bull. 36 (2001) 799–810.
[13] N.T. Silva, C.A. Bertran, M.A.S. Oliveira, G.P. Thim, J. Non-Cryst. Solids 304 (2002) 31–35.
[14] C.A. Bertran, N.T. da Silva, G.P. Thim, J. Non-Cryst. Solids 273 (2000) 140–144.
[15] A.M. Menchi, A.N. Scian, Mater. Lett. 59 (2005) 2664–2667.
[16] M. Majumder, S. Mukhopadhyay, O. Parkash, D. Kumar, Ceram. Int. 30 (2004) 1067–1070.
[17] A. Yamuna, S. Honda, K. Sumita, M. Yanagihara, S. Hashimoto, H. Awaji, Micropor. Mesopor. Mater. 85 (2005) 169–175.
[18] I. Jankovic-Castvan, S. Lazarevic, D. Tanaskovic, A. Orlovic, R. Petrovic, D. Janackovic, Ceram. Int. 33 (2007) 1263–1268.
[19] M. Angeles, J.A. Villegas, J. Eur. Ceram. Soc. 22 (2002) 487–494.
[20] J. Francisco, J.A. Torres, J. Eur. Ceram. Soc. 24 (2004) 681–691.
[21] S.-H. Lo, C.-F. Yang, Ceram. Int. 24 (1998) 139–144.
[22] D.C.V.A.D.T. Weaver, J.D. Smith, J. Mater. Sci. 39 (2004) 51–59.
[23] A. Goel, E.R. Shaaban, F.C.L. Melo, M.J. Ribeiro, J.M.F. Ferreira, J. Non-Cryst. Solids 353 (2007) 2383–2391.
[24] S. Wang, H. Zhou, L. Luo, Mater. Res. Bull. 38 (2003) 1367–1374.
[25] G.-H. Chen, J. Alloys Compd. 455 (2008) 298–302.
[26] B.H. Kim, K.H. Lee, J. Mater. Sci. 29 (1994) 6592–6598.
[27] P. Amista, M. Cesari, A. Montenero, G. Gnappi, L. Luo, J. Non-Cryst. Solids 192–193 (1995) 529–533.
[28] G.-H. Chen, X.-Y. Liu, J. Alloys Compd. 431 (2007) 282–286.
[29] N.J. Azin, M.A. Camerucci, A.L. Cavalieri, Ceram. Int. 31 (2005) 189–195.
[30] A.G. Gregory, T.J. Veasey, J. Mater. Sci. 8 (1973) 324–332.
[31] I. Jankovic-Castvan, S. Lazarevic, B. Jordovic, R. Petrovic, D. Tanaskovic, D. Janackovic, J. Eur. Ceram. Soc. 27 (2007) 3659–3661.
[32] M.S. Jogad, M.G.A. Sarkar, T. Mirza, L.A. Udachan, G.P. Kothiyal, Mater. Lett. 57 (2002) 619–627.
[33] M.A. Camerucci, G. Urretavizcaya, M.S. Castro, A.L. Cavalieri, J. Eur. Ceram. Soc. 21 (2001) 2917–2923.
[34] T.S. Sasikala, M.N. Suma, P. Mohanan, C. Pavithran, M.T. Sebastian, J. Alloys Compd. 461 (2008) 555–559.
[35] B.P. Kumar, H.H. Kumar, D.K. Kharat, Mater. Sci. Eng. B 127 (2006) 130–133.
[36] J. Banjuraizah, H. Mohamad, Z.A. Ahmad, J. Alloys Compd. 482 (2009) 429–436.
[37] M.N. Rahaman, Ceramic Processing and Sintering, Marcel Dekker Inc., New York, 2003.
[38] P.W. McMillan, Glass–Ceramics, Academic Press Inc., London, 1969.